Toward the Oxidation of the Phenyl Radical and Prevention of PAH Formation in Combustion Systems

Dorian S. N. Parker, Ralf. I. Kaiser*

Department of Chemistry, University of Hawaii at Manoa, Honolulu, HI 96822, USA

Tyler P. Troy, Oleg Kostko, Musahid Ahmed*

Chemical Sciences Division, Lawrence Berkeley National Laboratory, Berkeley, CA 94720, USA

Alexander M. Mebel*

Department of Chemistry and Biochemistry, Florida International University, Miami, FL 33199, USA

Abstract

The reaction of the phenyl radical (C_6H_5) with molecular oxygen (O_2) plays a central role in the degradation of poly- and mono- cyclic aromatic radicals in combustion systems which would otherwise react with fuel components to form polycyclic aromatic hydrocarbons (PAH) and eventually soot. Despite intense theoretical and experimental scrutiny over half a century, the overall reaction channels have not all been experimentally identified. Tunable vacuum ultraviolet photoionization in conjunction with a combustion simulating chemical reactor uniquely provides the complete isomer specific product spectrum and branching ratios of this prototype reaction. In the reaction of phenyl radicals and molecular oxygen at 873 K and 1,003 K, ortho-benzoquinone (*o*-$C_6H_4O_2$), the phenoxy radical (C_6H_5O), cyclopentadienyl radical (C_5H_5), were identified as primary products formed through emission of atomic hydrogen, atomic oxygen and carbon dioxide. Furan (C_4H_4O), acrolein (C_3H_4O) and ketene (C_2H_2O) were also identified as primary products formed through ring opening and fragmentation of the 7-membered ring 2-oxepinoxy radical. Secondary reaction products para-benzoquinone (*p*-$C_6H_4O_2$), phenol (C_6H_5OH), cyclopentadiene (C_5H_6), 2,4-cyclopentadienone (C_5H_4O), vinylacetylene (C_4H_4), and acetylene (C_2H_2) were also identified. The pyranyl radical (C_5H_5O) was not detected, however, electronic structure calculations show that it is formed and isomerizes to 2,4-cyclopentadienone through atomic hydrogen emission. In combustion systems, barrier-less phenyl-type radical oxidation reactions could even degrade more complex aromatic radicals. An understanding of these elementary processes is expected to lead to a better understanding toward the elimination of carcinogenic, mutagenic and environmentally hazardous byproducts of combustion systems such as polycyclic aromatic hydrocarbons (PAHs).

I. Introduction

The combustion of fossil fuel drives the economy of our planet and delivers energy by oxidation of aliphatic, alicyclic, and aromatic hydrocarbons. Ideally, this process leads solely to carbon dioxide (CO_2) and water (H_2O). However, in 'real' combustion systems, in competition with these oxidation reactions are formation routes to carcinogenic, mutagenic and environmentally detrimental species - polycyclic aromatic hydrocarbons (PAH)[1,2] - and soot particles.[3,4] These pathways involve reactions of resonantly stabilized free radicals (RSFRs) like propargyl (C_3H_3) and aromatic radicals (ARs) such as the phenyl radical with unsaturated hydrocarbons.[5,6,7] Alternatively, in combustion environments, phenyl radicals also react with molecular oxygen – a key reaction that removes these radicals from PAH formation routes. At temperatures higher than 1,000 K, this reaction is initiated by forming a rovibrationally excited peroxybenzene radical ($C_6H_5O_2$)* [**1**], that emits an oxygen atom leading to the phenoxy radical (C_6H_5O) [**2**].[8-11] The formation of the phenoxy radical (C_6H_5O) has also been observed as the primary product via crossed molecular beam experiments in the single collision regime at high temperatures.[12-14] Below 1,000 K, based on kinetics studies, it has been postulated, that an addition-stabilization process yields the peroxybenzene radical ($C_6H_5O_2$) as the primary product.[10] Theoretical investigations have predicted the isomerization of the peroxybenzene radical ($C_6H_5O_2$) with insertion of one of the oxygen atoms into the ring to form a seven-membered ring radical 2-oxepinoxy ($C_6H_5O_2$).[8,15,16] Kinetics experiments on the oxidation of phenyl radicals observed the formation of para-benzoquinone ($C_6H_4O_2$) [**3**] through atomic hydrogen emission.[17,18] Theoretical investigations predict further the formation of the cyclopentadienyl (c-C_5H_5) radical by carbon monoxide (CO) loss from the phenoxy radical [**4**][8,10] or through carbon dioxide (CO_2) emission [**5**] from benzoquinone.[19] Formation routes to pyranyl (c-C_5H_5O) plus carbon monoxide [**6**] and 2-oxo-2,3-dihydrofuran-4-yl (c-$C_4H_3O_2$) plus acetylene [**7**] through the decomposition of the seven-membered ring radical 2-oxepinoxy ($C_6H_5O_2$)[8,15] or via oxidation by another oxygen molecule[16] are also proposed. Ring opening of the 2-oxepinoxy radical ($C_6H_5O_2$) can form a 2,4-cyclopentadienone (c-C_5H_5O) radical by carbon monoxide (CO) emission [**8**].[15] The 2,4-cyclopentadienone (c-C_5H_5O) radical can emit a

hydrogen atom yielding 2,4-cyclopentadienone (C_5H_4O) [**9**]. From experimental studies of benzene oxidation using turbulent flow reactors, Glassman et al. proposed the observed 2,4-cyclopentadienone (C_5H_4O) was possibly from a secondary reaction of cyclopentadienyl with molecular oxygen.[20] The opening of the 2-oxepinoxy ($C_6H_5O_2$) ring leads to a number of linear dioxo radicals such as the 1,6-dioxo-3,5-hexadienyl ($C_6H_5O_2$) radical, which can subsequently fragment to yield polycarbon monoxides like 2-oxo-2,3-dihydrofuran-4-yl (C_4H_3O) and ketene (C_2H_2O) [**10**].[15] Emission of a C_2HO radical from 1,6-dioxo-3,5-hexadienyl ($C_6H_5O_2$) radical leads to furan (C_4H_4O) [**11**], or emission of carbon monoxide leads to a linear C_5H_5O molecule that subsequently fragments to a acrolein (C_3H_3O) radical plus acetylene [**12**]. Hydrogen addition to (C_3H_3O) or abstraction from another hydrocarbon can form the stable molecule acrolein (C_3H_4O). The fragmentation pattern continues for the polycarbon monoxide intermediates emitting a second carbon monoxide to form a C_4H_5 intermediate [**13**] that can then dissociate to acetylene (C_2H_2) and the vinyl radical (C_2H_3) [**14**],[15] or alternatively can emit a hydrogen atom to form vinylacetylene (C_4H_4) [**15**]. [21]

$C_6H_5 + O_2$	→	$C_6H_5O_2$*	[**1**]
$C_6H_5O_2$*	→	$C_6H_5O + O$	[**2**]
$C_6H_5O_2$*	→	$C_6H_4O_2 + H$	[**3**]
C_6H_5O	→	$C_5H_5 + CO$	[**4**]
$C_6H_5O_2$*	→	$C_5H_5 + CO_2$	[**5**]
$C_6H_5O_2$*	→	c-$C_5H_5O + CO$	[**6**]
$C_6H_5O_2$*	→	$C_4H_3O_2 + C_2H_2$	[**7**]
$C_6H_5O_2$*	→	l-$C_5H_5O + CO$	[**8**]
c-C_5H_5O	→	c-$C_5H_4O + H$	[**9**]
$C_6H_5O_2$*	→	$C_4H_3O + C_2H_2O$	[**10**]
$C_6H_5O_2$*	→	$C_4H_4O + C_2HO$	[**11**]
l-C_5H_5O	→	$C_3H_3O + C_2H_2$	[**12**]
l-C_5H_5O	→	$C_4H_5 + CO$	[**13**]
C_4H_5	→	$C_2H_2 + C_2H_3$	[**14**]
C_4H_5	→	$C_4H_4 + H$	[**15**]

Tokmakov et al. investigated the $C_6H_5O_2$ potential energy surface (PES) to provide a comprehensive view of the multiple reaction channels investigated for the phenyl plus molecular oxygen reaction, .[9] The authors proposed that feasible reaction pathways exist to the following products, phenoxy radical (C_6H_5O), benzoquinone (*p*-/*o*-$C_6H_4O_2$), the cyclopentadienyl radical (C_5H_5), pyranyl (C_5H_5O), and 2-oxo-2,3-dihydrofuran-4-yl (C_4H_3O). The most recent RRKM-ME calculations of product branching ratios in the temperature range of 1500-2500 K and pressures from 0.01 to 10 atm showed that the dominant reaction channel (>82%) leads to the

phenoxy radical product and its contribution increases with temperature. Chemically-activated phenoxy radical either decomposes to the cyclopentadienyl plus CO or undergoes thermal equilibration, where the relative yields of the decomposition/equilibration products strongly depend on temperature and pressure, with a temperature growth favoring decomposition and an increase in pressure favoring equilibration. At lower temperatures, the reaction was also predicted to yield significant amounts of pyranyl (C_5H_5O) plus CO, cyclopentadienyl (C_5H_5) plus CO, and o-benzoquinone (*o*-$C_6H_4O_2$) plus H. [22] However, despite the importance of the title reaction in combustion chemistry as a de-facto PAH inhibitor, these predictions have not been verified experimentally. This is mainly due to the difficulties in probing *all* reaction products simultaneously. Therefore, a comprehensive experimental determination of the degradation pathways of the phenyl radical by molecular oxygen has remained elusive to date.

In this article, we present the results of the multi-channel reaction of the phenyl radical with molecular oxygen explored experimentally under simulated combustion conditions. By exploiting the versatile detection technique of fragment-free single photon ionization coupled with mass spectroscopic detection of the photoionized products,[23-27] this study provides compelling evidence for the formation of primary reaction products [*o*-benzoquinone ($C_6H_4O_2$), the cyclopentadienyl radical (C_5H_5), and the phenoxy radical (C_6H_5O), furan (C_4H_4O), acrolein (C_3H_4O) and ketene (C_2H_2O)] and higher order products [*p*-benzoquinone ($C_6H_4O_2$), phenol (C_6H_5OH), cyclopentadiene (C_5H_6), 2,4-cyclopentadienone (C_5H_4O), vinylacetylene (C_4H_4), and acetylene (C_2H_2)]. This reaction represents the prototype system of a whole reaction class, in which aromatic radicals can be degraded via reactions with molecular oxygen in combustion systems eventually leading to an understanding of the elimination of toxic PAHs in the combustion of fossil fuel.

II. Experimental

The experiments were conducted at the Chemical Dynamics Beamline (9.0.2.) at the Advanced Light Source (ALS) exploiting a resistively heated high temperature 'chemical reactor' incorporated into a molecular beam vacuum chamber equipped with a Wiley-McLaren Reflectron Time-of-Flight mass spectrometer (ReTOF).[23-27] Phenyl radicals were generated *in situ* under combustion relevant conditions (temperature, pressure) via pyrolysis of nitroso-benzene (C_6H_5NO; Aldrich; 99.5+ %) seeded at levels of less than 0.1 % in molecular oxygen

(O_2; Praxair; 99.99 %) by expanding the mixture at a backing pressure of about 300 Torr through a 0.1 mm orifice via a resistively heated silicon carbide (SiC) tube (1 mm inner diameter) operating at 873 and 1,003 ± 150 K. The residence time of the phenyl radical and oxygen reactants within the tube was determined to be 26 ± 3 μs. Note that molecular oxygen acts not only as a seeding gas, but also as a reactant with the pyrolytically generated phenyl radicals. The continuous molecular beam generated in this process passes a 2 mm diameter skimmer located 10 mm downstream; this supersonic beam enters then the detection chamber, which houses the ReTOF mass spectrometer. Quasi-continuous tunable vacuum ultraviolet (VUV) radiation from the ALS interrogates the neutral molecular beam in the extraction region of the ReTOF mass spectrometer 55 mm downstream from the heated nozzle. Note that photo ionization via VUV radiation benefits from quasi *fragment free* ionization - a soft ionization method compared to traditional electron impact ionization. The ions generated are extracted and directed toward the ReTOF, which houses a microchannel plate detector (MCP). Signal from the MCP is digitized using a multichannel scaler. Photoionization efficiency (PIE) curves were obtained by integrating the signal collected at a specific mass-to-charge (m/z) selected for the species of interest over the range of photon energies from 8.00 eV to 11.00 eV in 0.05 eV increments and normalized to the photon flux.

III. Results

For the reaction of phenyl radicals with molecular oxygen, a characteristic mass spectrum collected at 10.50 eV is shown in Figure 1(A) for reactions conducted at 873 K and Figure 1(B) for 1003 K. The nozzle was run at an oxygen backing pressure of 300 Torr. The mass spectra depict product peaks at m/z 26 ($C_2H_2^+$), 42 ($C_2H_2O^+$), 52 ($C_4H_4^+$), 56 ($C_3H_4O^+$), 65 ($C_5H_5^+$), 66 ($C_5H_6^+$), 68 ($C_4H_4O^+$), 80 ($C_5H_4O^+$), 93 ($C_6H_5O^+$), 94 ($C_6H_6O^+$), and 108 ($C_6H_4O_2^+$). Blank spectra were recorded for neat nitrosobenzene and oxygen, respectively, in separate experiments and exhibit none of the peaks identified as products in the phenyl – oxygen experiment. The corresponding photoionization efficiency curves (PIE) for the products are shown in Figure 2 and 3 for the 873 K and 1003 K experiments respectively, reporting the intensities of the specific ion versus the photon energy. Each PIE depicted in Figure 2 and 3 by the black line is the average of three separate PIE scans, along with a shaded area indicating the error boundaries.

In the 873 K and 1003 K experiments, signal at m/z 108 are reflected in PIE curves (Figure 2A, 3A) that are well matched by a composite of reference PIE curves (purple line) for p-benzoquinone (blue line),[28] o-benzoquinone (red line),[28] and the ^{13}C counterpart of the parent molecule nitrosobenzene (green line) that is also observed at m/z 107 (Figure 1A). Under our experimental conditions for the 873 K experiment, the parent is not fully pyrolyzed as seen from the mass peak at m/z 107; a fraction of the signal at 108 originates from ^{13}C nitrosobenzene ($^{13}CC_5H_5NO$). In the 1003 K experiment the parent is almost fully pyrolyzed and the fit is achieved with no contribution from ^{13}C nitrosobenzene ($^{13}CC_5H_5NO$). The PIEs for m/z 94 and 93 (Figures 2B,3B and 2C,3C) are well matched by the PIE for phenol (C_6H_5OH) [29] and by the phenoxy radical (C_6H_5O), respectively. In the present study, the phenoxy radical reference PIE was obtained by generating the radical through pyrolysis of allyl phenyl ether ($C_3H_5OC_6H_5$) at 300 Torr and 873 K - a formation route to the phenoxy radical that has been well-documented.[30] The PIE of m/z 80 (Figure 2D,3D) is a very good match to the calculated PIE for 2,4-cyclopentadienone (C_5H_4O).[29] The signal at m/z 68 (Figure 2E,3E) although weak could be fit with experimental reference PIE's for furan (C_4H_4O).[31]

In the 873 K experiment, signal at m/z 65 (Figure 2G) has been assigned to the cyclopentadienyl radical (c-C_5H_5) due to its good match with the experimental reference PIEs (red line)[32] after subtraction of a dissociative ionization signal.[33] The raw PIE for m/z 65 depicted a strong exponential increase at about 10 eV, which for a hydrocarbon reactant with molecular formula C_5H_5 is an unfeasibly high ionization energy and therefore indicates dissociative ionization. The dissociative ionization of phenoxy radical forming cyclopentadienyl has been reported in the photodissociation of anisole to form phenoxy radicals.[33] We found that in the pyrolysis of allylphenyl ether to form the phenoxy radical, a signal at m/z 65 is observed with an onset at about 10 eV and depicts a strong exponential increase. The PIE shown in figure 2G is the result of subtraction of this exponential rise at 10 eV, found in the generation of the phenoxy radical from allylphenyl ether pyrolysis, from the raw PIE collected from the reaction of phenyl with molecular oxygen. In the 1003 K experiment the phenoxy radical contribution is significantly reduced, while the cyclopentadienyl signal significantly increased. As a result no dissociative ionization signal was found at 10 eV and the PIE shown in Figure 3G is a good fit to the reference PIE for cyclopentadienyl radical (c-C_5H_5) (red line).[32] The pent-1-en-4-yn-3-yl

radical (65 amu), which has a PIE onset of 7.88 eV, is clearly not formed under our experimental conditions.[29]

In the 873 K experiment, the PIE at m/z 66 (Figure 2F) is attributed to cyclopentadiene (c-C_5H_6) as shown by the match to its experimental reference PIE (red lines).[32] In a similar fashion to the cyclopentadienyl (C_5H_5) spectrum at m/z 65, the raw PIE for m/z 66 shows a marked increase in photoioinization efficiency slightly below 10 eV. We attribute this same characteristic PIE rise to dissociative ionization that is seen in the m/z 66 signal in the pyrolysis of allylphenyl ether generating the phenoxy radical. Figure 2F shows the PIE at m/z 66 after subtraction of this dissociative ionization signal. In the 1003 K experiment, there was also a small dissociative ionization contribution to the signal at m/z 66, and subsequently subtracted from it. Here, the cyclopentadiene signal is of a similar magnitude to phenoxy radical and therefore could be expected to contribute to the signal. The resulting PIE at m/z 66 is shown in Figure 3F and is well fit by cyclopentadiene (c-C_5H_6) experimental reference PIE (red line).[32] It should be noted that 1,2,4-pentatriene with an ionization energy of 8.88 eV does not contribute to either signal. The linear molecules pent-3-yne and 3-pent-1-yne (l-C_5H_6) have similar PIE onset as the signal at m/z 66 but quickly plateau at 8.90 eV, and therefore do not fit.

Finally, the PIE at m/z 52 (Figure 2H, 3H) are well matched with the reference spectrum for vinylacetylene (C_4H_4),[34] and the PIE at m/z 53 is the ^{13}C signal of vinylacetylene (C_4H_4) with no contribution from C_4H_5. The PIE at m/z 42 (Figure 2I, 3I) matches the reference PIE for ketene (C_2H_2O)[31] and the PIE collected at m/z 26 (Figure 2K, 3K) shows good agreement with the reference PIE for acetylene (C_2H_2).[31] The PIE of the signal at m/z 56 (Figure 2J, 3J) are well matched by the PIE of acrolein (C_3H_4O) (red line).[35] The branching ratios percentage for each product peak (m/z = 108, 94, 93, 80, 68, 66, 65, 56, 52, 42 and 26) have been calculated along with error bars and shown in Table 1 and in Figure 4 for the reaction of phenyl radicals and molecular oxygen at 873 K and 1003 K. The branching ratios were calculated based on integrated mass peaks primarily from the mass spectra depicted in Figure 1 at 10.5 eV. In the case of acetylene mass spectra at 12 eV was used along with the strong signal of vinylacetylene as a reference. The absorption cross sections used are referenced in Table 1.

IV. Discussion

Having identified the products formed in the elementary reaction of the phenyl radical with molecular oxygen, we will now rationalize their formation pathways and propose a reaction mechanism (Figure 3). Initially a peroxybenzene radical intermediate is formed via a barrier-less addition of the phenyl radical to molecular oxygen. From peroxybenzene, the terminal peroxide oxygen migrates to the *ortho* carbon, from which a hydrogen atom is emitted to form o-benzoquinone.[9] Further migration of the oxygen atom to the para position leading to the formation of p-benzoquinone is practically negligible according to calculations.[9] Furthermore, by this mechanism we would also expect to see formation of m-benzoquinone. Therefore, formation of p-benzoquinone is associated with a secondary reaction. The second pathway available to peroxybenzene involves an atomic oxygen emission to form the phenoxy radical. The phenoxy radical has been observed experimentally in single collision crossed beam reactions[12-14] and predicted as the primary reaction product theoretically, especially when approaching high temperatures of 1,500 K – 2,500 K.[8-10] Finally, peroxybenzene can isomerize to 2-oxepinoxy radical and subsequently emit a carbon dioxide molecule to form the cyclopentadienyl radical (C_5H_5). Electronic structure calculations predict the cyclopentadienyl radical can be reached by a number of pathways, the two lowest energy pathways pass through the seven-membered ring intermediate 2-oxepinoxy before undergoing rearrangement and carbon dioxide emission.[9] The formation of cyclopentadienyl radical by carbon dioxide emission is calculated to be the most exoergic reaction channel ranging from 480 kJ mol^{-1} below the energy of the reactants. The cyclopentadienyl radical is also accessible through a carbon monoxide (CO) emission from the phenoxy radical. Here, the ring structure is formed before carbon monoxide emission in a series of increasingly endoergic isomerization steps resulting in a reaction energy of 38 kJ mol^{-1} above the energy of the reactants.[36,37] The 2-oxepinoxy radical can undergo ring rupture to form a 1,6-dioxo-3,5-hexadienyl radical intermediate which can subsequently dissociate to form a range of polycarbon monoxide molecules and radicals.[15] These in turn can fragment further or undergo hydrogen addition or abstract a hydrogen atom.[15] Calculations show that 1,6-dioxo-3,5-hexadienyl radical intermediate can cyclize to furan (C_4H_4O) and emit a ketene (C_2HO) radical or emit carbon monoxide, then fragment to acetylene and the acrolein radical (C_3H_3O).[15] The ketene and acrolein radicals can easily undergo hydrogen atom addition or abstract one from another molecule as seen with the phenoxy and cyclopentadienyl radicals forming phenol and

cyclopentadiene, to form ketene (C_2H_2O) and acrolein (C_3H_4O), respectively. The fragmentation of the 1,6-dioxo-3,5-hexadienyl radical and 2-oxepinoxy radicals can form furan (C_4H_4O), ketene (C_2H_2O) and acrolein (C_3H_4O) directly along with a radical counterpart, and are therefore considered primary reaction products. To conclude, the primary products formed in the reaction of phenyl radical with molecular oxygen are *o*-benzoquinone plus atomic hydrogen [**3**], the phenoxy radical plus atomic oxygen [**2**], cyclopentadienyl radical plus carbon dioxide [**5]**, C_4H_3O plus ketene [**11**], acrolein plus carbon monoxide and acetylene and furan plus ketene radical [**11**].

Having established the primary reaction products, we now explore the potential formation pathways to *secondary and/or higher order products*. The phenoxy radical has resonant structures with carbon centered radicals, of which the para-carbon centered radical would be the most stable.[38,39] Reaction of a *para*-carbon centered phenoxy radical with molecular oxygen followed by oxygen and hydrogen atom emissions could account for *para*-benzoquinone formation. The formation of phenol can be explained via hydrogen atom addition to the phenoxy radical; alternatively, the phenoxy radical can abstract a hydrogen atom from any hydrogen-bearing species. Previous combustion experiments found phenol formation whenever phenoxy radicals are generated.[40] The cyclopentadienyl radical can also undergo a hydrogen addition and/or abstraction to form cyclopentadiene.[17] The formation of 2,4-cyclopentadienone (C_5H_4O) might be due to secondary decomposition of pyranyl as will be discussed later, and is accessible through the reaction of cyclopentadienyl with atomic oxygen followed by atomic hydrogen loss or via the decomposition of benzoquinone through carbon monoxide emission which has been seen for p-benzoquinone decomposition.[17]

The final series of reactions involve carbon monoxide emission and/or ring openings to yield acyclic unsaturated hydrocarbons such as vinylacetylene (C_4H_4) and acetylene (C_2H_2). Glassman et al. predicted that 2,4-cyclopentadienone (C_5H_5O) radical can undergo decomposition via carbon monoxide emission to form a butadienyl radical (C_4H_5), which then emits a hydrogen atom to form vinylacetylene.[20] The butadienyl radical intermediate can also dissociate via carbon-carbon cleavage to form acetylene plus a vinyl radical.[20] It should be noted the mass peak at m/z 53 was solely from ^{13}C isotope of vinylacetylene m/z 52 and not from the butadienyl radical. Acetylene can undergo addition by an oxygen atom to form ketene. We did not observe

pyranyl (C_5H_5O) plus carbon monoxide [**6**] or 2-oxo-2,3-dihydrofuran-4-yl (c-$C_4H_3O_2$) plus acetylene [**7**] reaction channels under our experimental conditions of 873 K and 1003 K at 300 Torr. The pathway to 2-oxo-2,3-dihydrofuran-4-yl was predicted to be uncompetitive by the theoretical calculations.[9,22] On the contrary, the yield of pyranyl was anticipated to increase as the temperature decreases below 1500 K and hence be significant under the conditions of the present experiment. In order to explain the non-observation of pyranyl, we computed its secondary decomposition pathway using the quantum chemical CCSD(T)/CBS(dtq)//B3LYP/6-311G** method. The potential energy diagram is illustrated in Figure 6. One can see that pyranyl first undergoes ring contraction to a five-member ring structure via an epoxy-like intermediate and then loses an H atom to form 2,4-cyclopentadien-1-one after a hydrogen migration from C(O) to C(H). While the overall decomposition reaction is computed to be endothermic by 177 kJ mol^{-1}, the highest barrier on this pathway is at 186 kJ mol^{-1} above pyranyl. Meanwhile, the exothermicity of the $C_6H_5 + O_2 \rightarrow$ pyranyl + carbon monoxide channel was computed to be as high as 379 kJ mol^{-1}.[9] If the primary pyranyl fragment is formed with that internal energy, its lifetime with respect to the decomposition to 2,4-cyclopentadien-1-one is computed to be only 0.3 ns using RRKM theory. The most probable kinetic energy of the primary fragments should resemble the reverse barrier height at the last step of decomposition of a $C_6H_5O_2$ intermediate to pyranyl plus carbon monoxide , which is 85 kJ mol^{-1} according to the earlier calculations.[9] If we subtract this energy from the reaction exothermicity and assume that most of the available energy should be transferred to the internal energy of the larger pyranyl fragment, the energy available to pyranyl then would be 294 kJ mol^{-1}. In this case, the computed lifetime increases to 6 ns, which is still more than three orders of magnitude shorter than the residence time in the tube. Although some fraction of pyranyl molecules may be deactivated by collisions and thus survive longer, according to the experimental data, this fraction is not sufficient enough to be detected.

The branching ratios depicted in figure 4 and listed in Table 1 deliver the relative weighting of decomposition pathways shown in figure 5 and an insight into the role temperature plays in their determination. Although these data cannot provide quantitative information on the reaction mechanisms, we will briefly discuss the observed trends qualitatively and speculate on their origins. Overall, the 873 K experiment shows higher levels of high mass products, while the 1003 K experiment show an increase in lower mass products starting at the cyclopentadienyl radical (m/z 65). Most likely, the reaction mechanism is being pushed down to low mass

products through an increased amount of decomposition and fragmentation. The low temperature experiment at 873 K provides a snapshot of the mechanism before reaching the final products. Interestingly, the cyclopentadienyl signal increases proportionately to the decrease in the phenoxy signal, indicating that although phenoxy is formed at higher temperatures it almost immediately decomposes to cyclopentadienyl and other products. The branching ratios of o-benzoquinone are about 0.25 of those of p-benzoquinone indicating that the formation of the phenoxy radical by oxygen emission is preferential to formation of o-benzoquinone by hydrogen emission. The branching ratios of both benzoquinone isomers get proportionately lower with increasing temperature, a likely indicator of their thermal lability. The 2,4-cyclopentadiene-1-one signal shows about the same decrease of 0.5 with increased temperature as o-benzoquinone, indicating these pathways may be coupled as shown in figure 5. Alternatively, this observation corroborates the hypothesis that 2,4-cyclopentadiene-1-one is largely produced via secondary decomposition of pyranyl because the primary yields of o-benzoquinone and pyranyl show similar trends decreasing with temperature according to the RRKM-ME calculations.[22] Furan depicts a decrease with increased temperature, indicating it breaks down further at higher temperatures and is a primary product. Likewise, ketene shows a minimal relative rise with increased temperature. Acrolein on the other hand rises by a factor of 2.5 and most likely represents a terminal product of the reaction. Vinylacetylene shows only a marginal increase with temperature while acetylene shows a greater increase. Vinylacetylene is a dominant product in the phenyl plus oxygen reaction which may well be being degraded further to acetylene with increased temperature.

V. Conclusion

A high temperature chemical reactor was exploited to comprehensively investigate the primary and secondary products of the multi-channel reaction of the phenyl radical with molecular oxygen under combustion relevant conditions (300 Torr, 873 K and 1003 K) exploiting fragment-free photoionization of the neutral products. The formation of the primary products is initiated by the addition of molecular oxygen to the phenyl radical; the peroxybenzene radical intermediate reacts via three pathways ultimately forming: i) *o*-benzoquinone ($C_6H_4O_2$), ii) the cyclopentadienyl radical (C_5H_5), iii) the phenoxy radical (C_6H_5O), iv) furan (C_4H_4O), v) acrolein (C_3H_4O) and vi) ketene (C_2H_2O). Higher order reaction

products phenol (C_6H_5OH) and cyclopentadiene (C_5H_6) are formed through a barrier-less atomic hydrogen addition to the phenoxy and cyclopentadienyl radical, respectively. 2,4-cyclopentadienone (C_5H_4O) may originate from decomposition of an unobserved primary fragment pyranyl (C_5H_5O), or from cyclopentadienyl addition to either atomic or molecular oxygen followed by emission of atomic hydrogen or OH (or atomic oxygen followed by atomic hydrogen), respectively, or through carbon monoxide emission from *o*-/*p*-benzoquinone. 2,4-cyclopentadienone presents the central reaction intermediate leading to highly unsaturated carbons as the 2,4-cyclopentadienone radical degrades to vinylacetylene (C_4H_4) through sequential carbon monoxide and atomic hydrogen yielding eventually vinylacetylene and acetylene. We find no evidence of pyranyl (C_5H_5O) formation, which may be due to its fast secondary decomposition to 2,4-cyclopentadienone plus H.

Our results on the reaction of the phenyl radical with molecular oxygen – the prototype system leading to the degradation of aromatic radicals - highlight the importance of universal detection techniques in identifying isomer-specific product distributions produced within combustion environments comprehensively, rather than only select products. This method allows for experimental identification of hitherto elusive products and the elucidation of complete reaction networks. We anticipate that the present study acts as a conceptual template to initiate further investigations into the degradation pathways of more complex aromatic radicals by molecular oxygen exploiting fragment-free tunable vacuum ultraviolet photoionization. These reactions could involve, for instance, – prototypes of bicyclic PAH radicals – the naphthyl ($C_{10}H_7$) and indenyl (C_9H_7) radicals. Additionally, this method could be expanded to more complex systems such as nitrogen-substituted PAH radicals of biological importance relevant to DNA and RNA damage by ionizing radiation.

Acknowledgements

This material is based upon work supported by the U.S. Department of Energy, Office of Science, DE-FG02-03ER15411 to the University of Hawaii and DEFG02-04ER15570 to FIU. The authors MA, OK and TPT, and the Advanced Light Source are supported by the Director, Office of Science, Office of Basic Energy Sciences, of the U.S. Department of Energy under Contract No. DE-AC02-05CH11231, through the Chemical Sciences Division.

Table 1. Branching Ratios of Species Formed in the reaction of Phenyl with Oxygen Utilizing a Chemical Reactor at 300 Torr, 873 K and 1003 K.

Mass-to-charge ratio	Name	Molecular Formula	Branching Ratio (%)		Fractional Change between 873 K and 1003 K
			873 K	1003 K	
108	o-Benzoquinone[28]	o-$C_6H_4O_2$	0.54 ± 0.01	0.21 ± 0.01	0.39
108	p-Benzoquinone[28]	p-$C_6H_4O_2$	2.62 ± 0.05	0.93 ± 0.02	0.35
94	Phenol[40]	C_6H_6O	10.99 ± 0.22	5.08 ± 0.10	0.46
93	Phenoxy[33]	C_6H_5O	25.16 ± 0.50	3.90 ± 0.08	0.16
80	2,4-Cyclopentadiene-1-one[29]	C_5H_4O	18.50 ± 0.18	9.04 ± 0.09	0.49
68	Furan[31]	C_4H_4O	4.48 ± 0.45	1.39 ± 0.14	0.31
66	1,3-Cyclopentadiene[31]	C_5H_6	4.87 ± 0.49	3.85 ± 0.38	0.79
65	Cyclopentadienyl[32]	C_5H_5	6.66 ± 0.83	30.47 ± 3.81	4.58
56	Acrolein[35]	C_3H_4O	6.00 ± 0.06	15.31 ± 0.15	2.55
52	Vinyacetylene[34]	C_4H_4	14.03 ± 0.14	17.88 ± 0.18	1.27
42	Ketene[31]	C_2H_2O	3.73 ± 0.11	5.27 ± 0.16	1.41
26	Acetylene[34]	C_2H_2	2.43 ± 0.02	6.68 ± 0.07	2.75

Figures

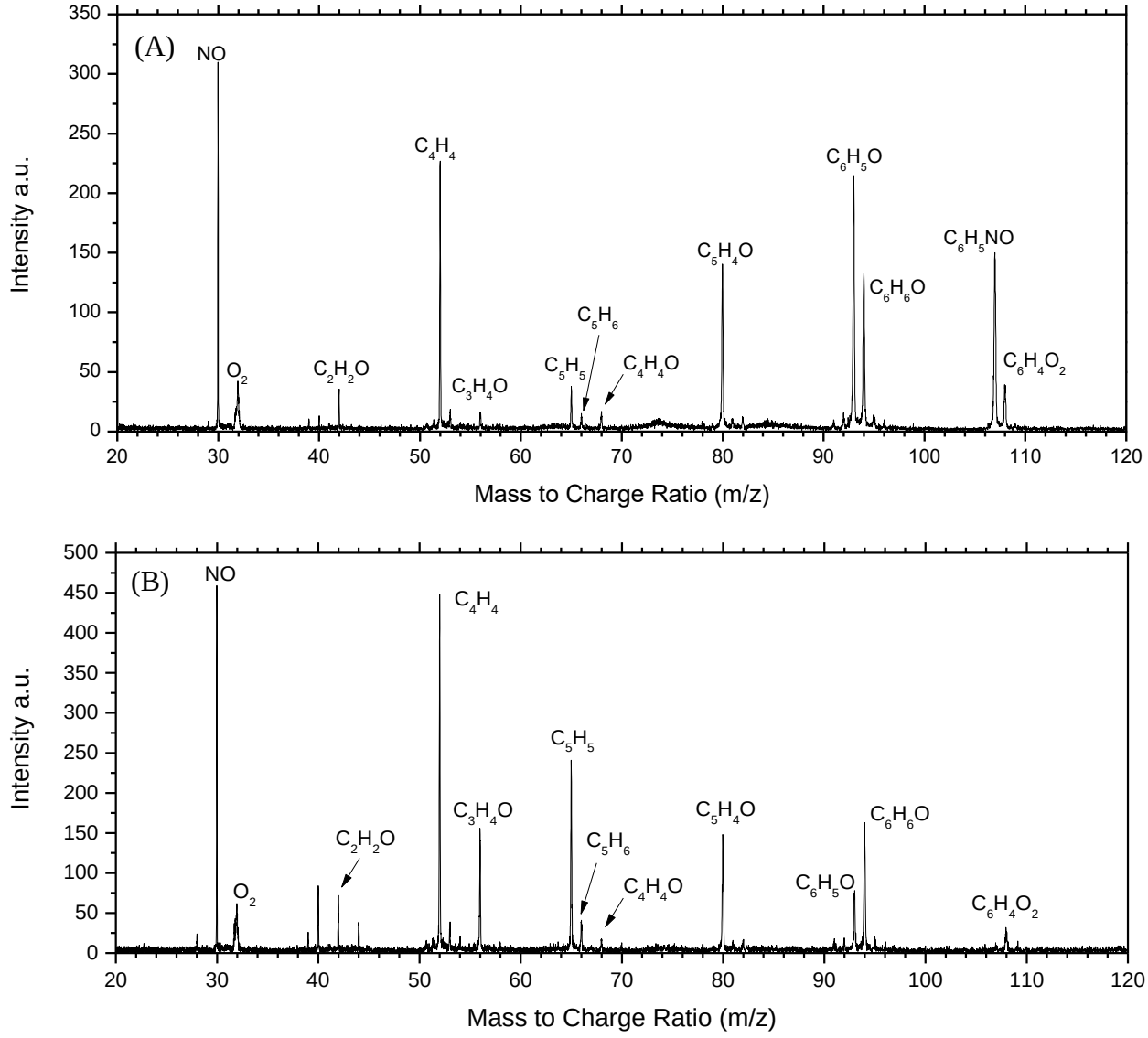

Figure 1: Mass spectrum of the products of the phenyl−oxygen pyrolytic reaction recorded at a photon energy of 10.50 eV, 873 K (A) and 1003 K (B).

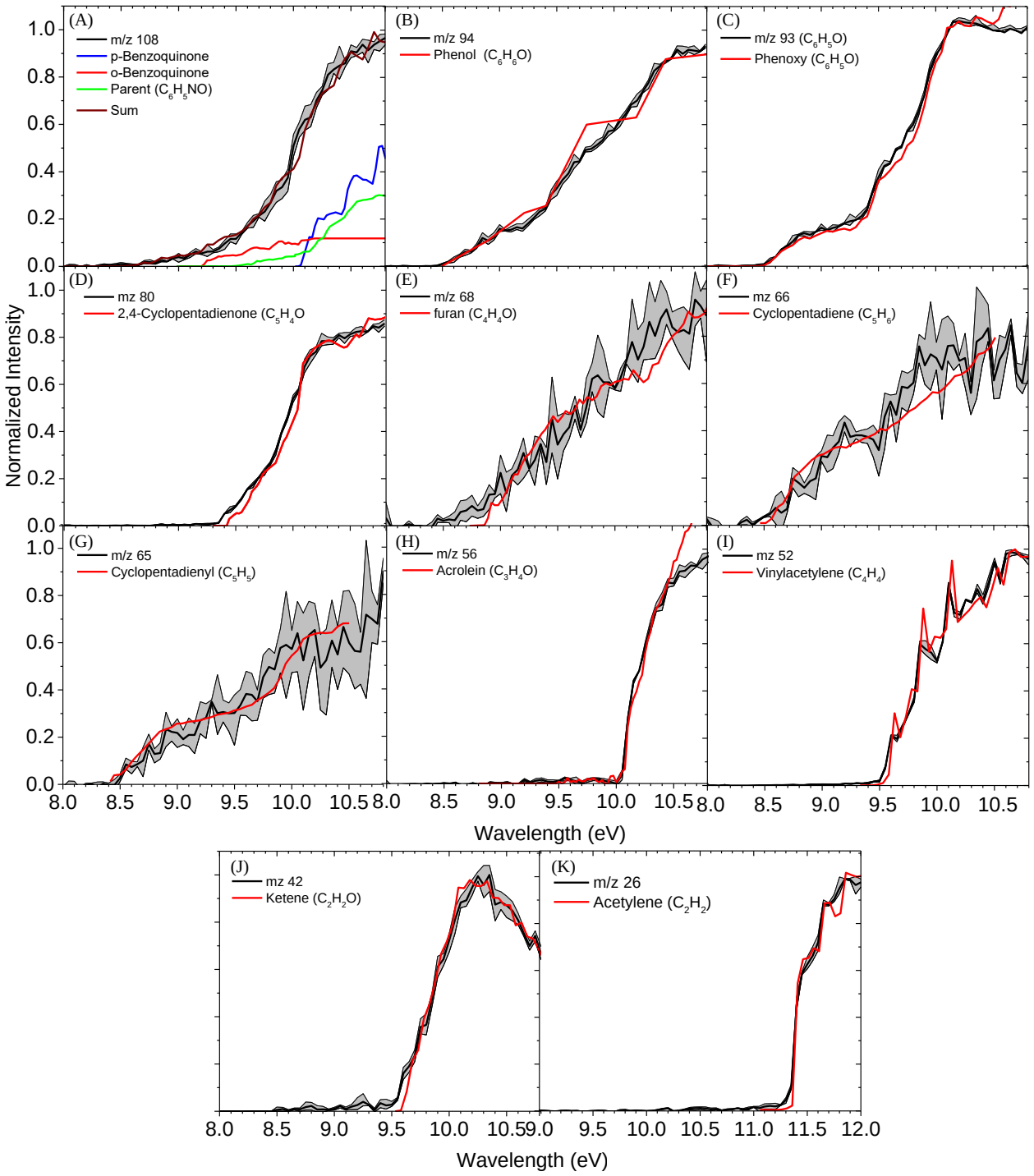

Figure 2: Experimentally obtained photoionization energy curve (PIE) recorded at 873 K at m/z = 108, 94, 93, 80, 68, 66, 65, 56, 52, 42 and 26, shown as black line along with experimental errors defined as the grey area. Reference PIE curves for each m/z ratio are shown as primary color (red, green, blue) lines with the sum of the composite PIEs as the brown line.

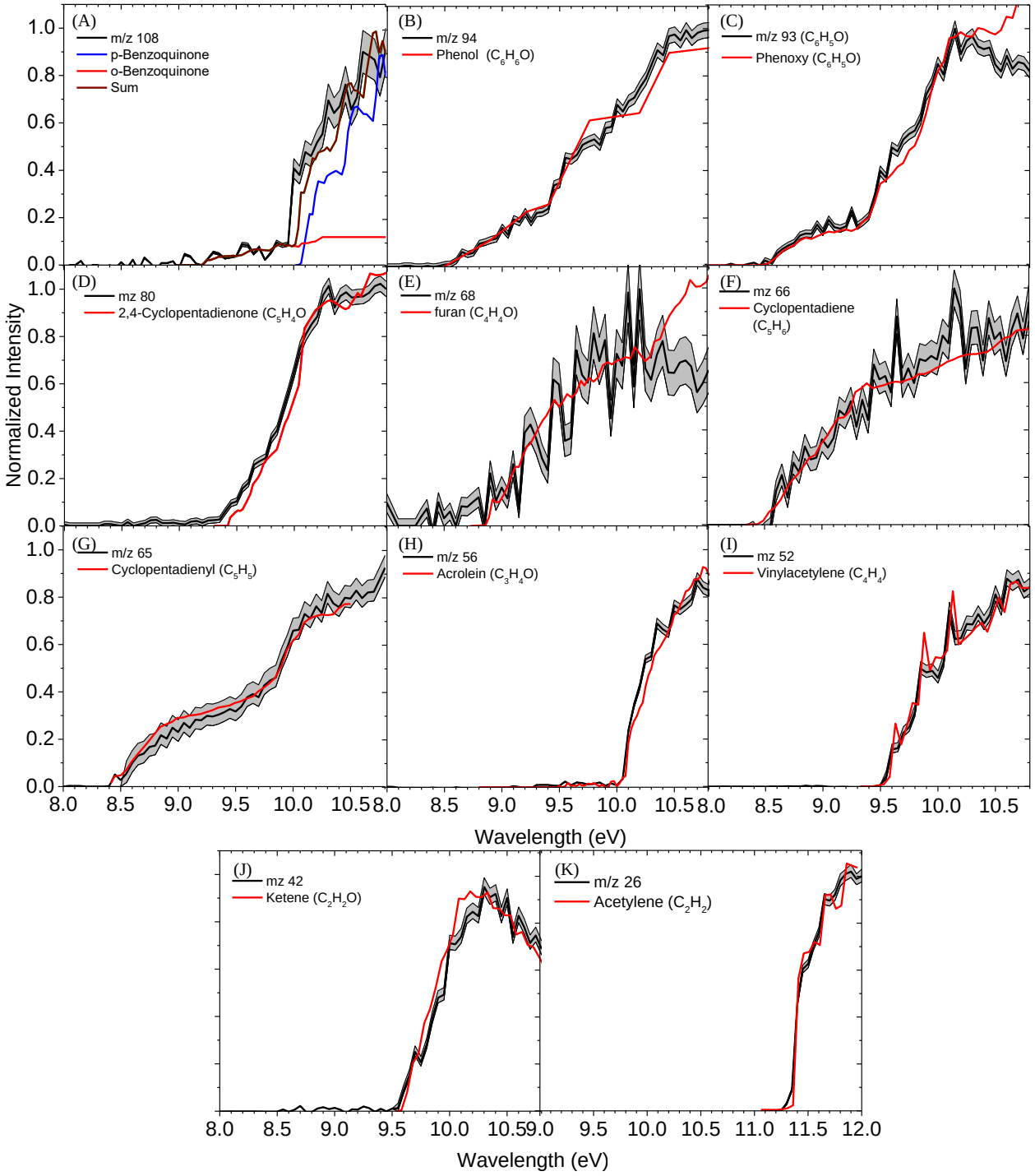

Figure 3: Experimentally obtained photoionization energy curve (PIE) recorded at 1003 K at m/z = 108, 94, 93, 80, 68, 66, 65, 56, 52, 42 and 26, shown as black line along with experimental errors defined as the grey area. Reference PIE curves for each m/z ratio are shown as primary color (red, green, blue) lines with the sum of the composite PIEs as the brown line.

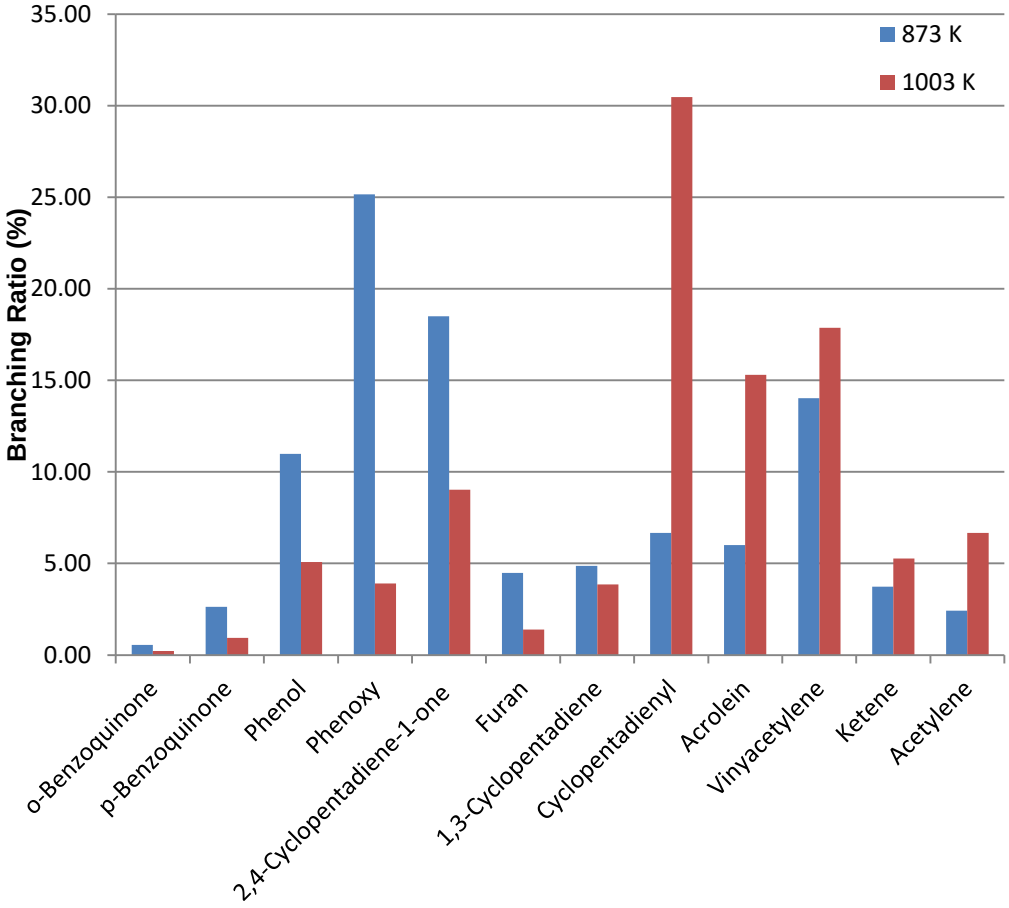

Figure 4: Branching ratio percentage for reaction of phenyl radicals with molecular oxygen at a pressure of 300 Torr at nozzle temperatures of 873 K (blue Column) and 1,003 K (red Column) as shown in Table 1.

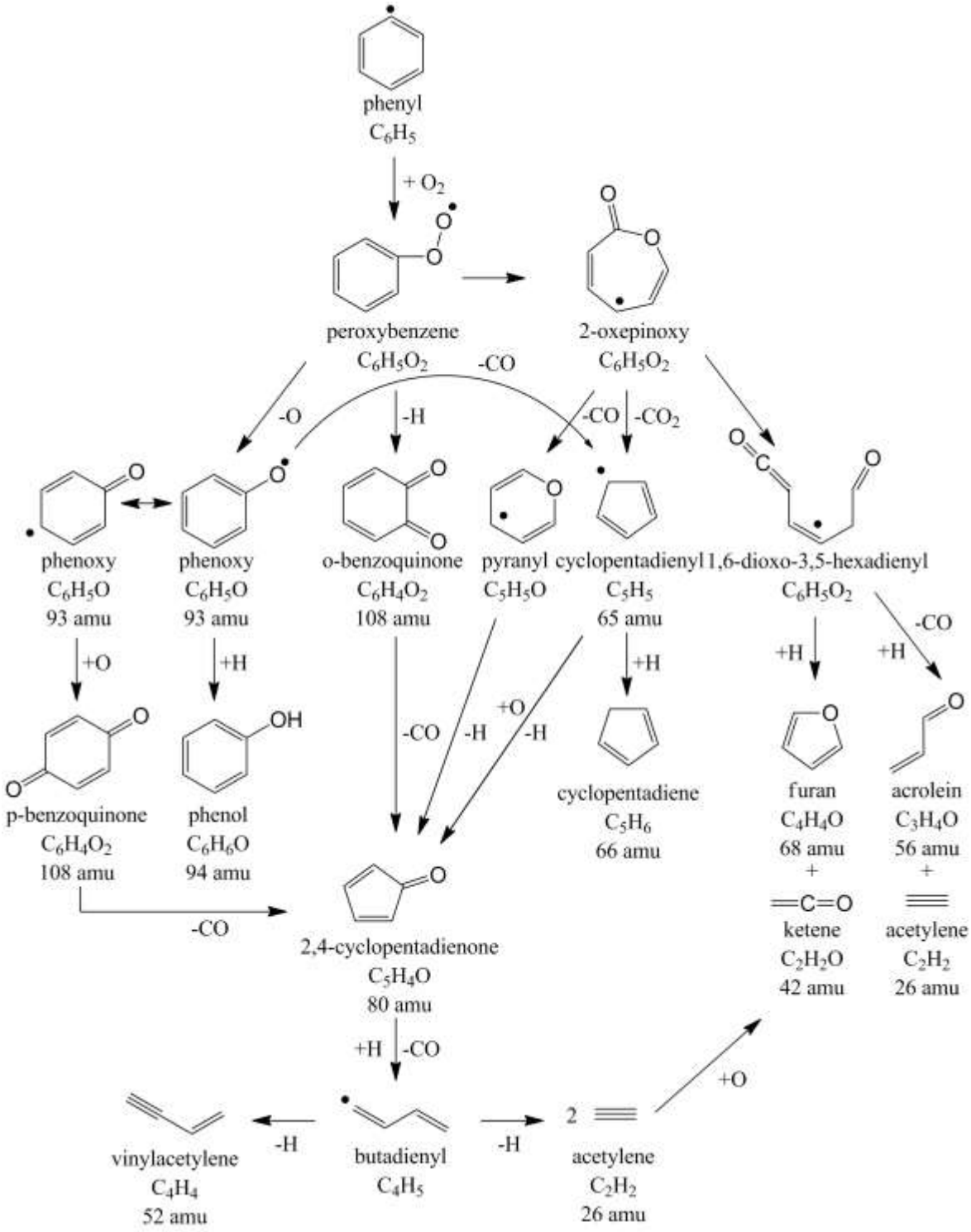

Figure 5: Proposed mechanism for products observed in the reaction of phenyl radicals with molecular oxygen at 300 Torr, 873 K and 1003 K. Masses in amu have been given for the species observed in the experiments. [9]

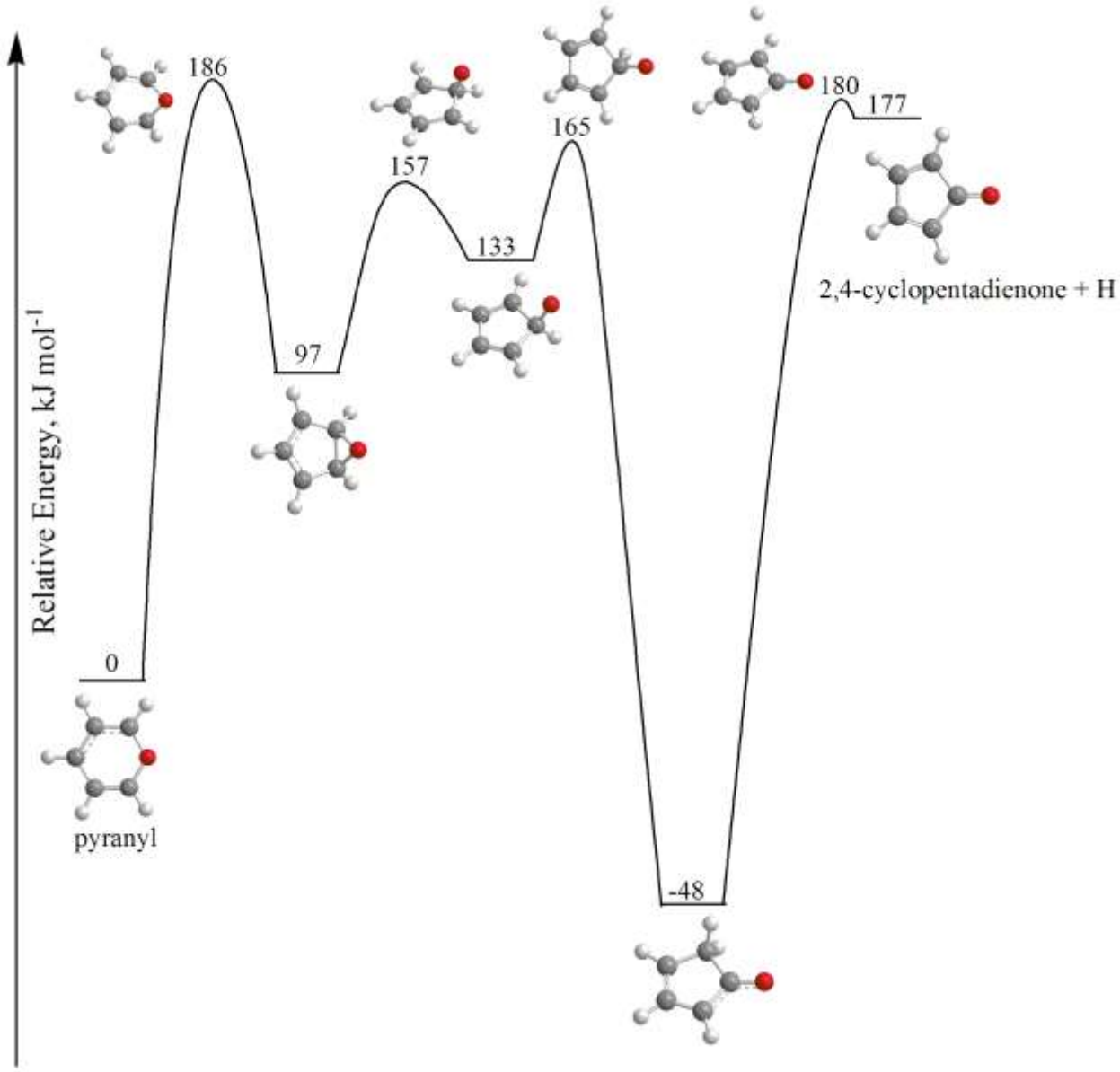

Figure 6. Potential energy diagram for decomposition of pyranyl to 2,4-cyclopentadienone + H calculated at the CCSD(T)/CBS(dtq)//B3LYP/6-311G** + ZPE(B3LYP/6-311G**) level of theory. Relative energies of various species are given in kJ mol^{-1}.

References

(1) Baird, W. M.; Hooven, L. A.; Mahadevan, B., *Environ. and Mol. Mut.*, **2005**, *45*, 106-114.

(2) Finlayson-Pitts, B. J.; Pitts, J. N., Jr., *Science*, **1997**, *276*, 1045-1052.

(3) Frenklach, M., *Phys. Chem. Chem. Phys.*, **2002**, *4*, 2028-2037.

(4) Richter, H.; Howard, J. B., *Phys. Chem. Chem. Phys.*, **2002**, *4*, 2038-2055.

(5) Parker, D. S. N.; Zhang, F.; Kim, Y. S.; Kaiser, R. I.; Landera, A.; Kislov, V. V.; Mebel, A. M.; Tielens, A. G. G. M., *Proc. Natl. Acad. Sci.*, **2012**, *109*, 53-58

(6) Kaiser, R. I.; Parker, D. S. N.; Zhang, F.; Landera, A.; Kislov, V. V.; Mebel, A. M., *J. Phys. Chem. A*, **2012**, *116*, 4248-4258.

(7) Parker, D. S. N.; Zhang, F.; Kaiser, R. I.; Kislov, V. V.; Mebel, A. M., *Chem.--Asian J.* , **2011**, *6*, 3035-3047.

(8) Barckholtz, C.; Fadden, M. J.; Hadad, C. M., *J. Phys. Chem. A*, **1999**, *103*, 8108-8117.

(9) Tokmakov, I. V.; Kim, G.-S.; Kislov, V. V.; Mebel, A. M.; Lin, M. C., *J. Phys. Chem.*, **2005**, *109*, 6114-6127.

(10) Yu, T.; Lin, M. C., *J. Am. Chem. Soc.*, **1994**, *116*, 9571-9576.

(11) Fadden, M. J.; Barckholtz, C.; Hadad, C. M., *J. Phys. Chem. A*, **2000**, *104*, 3004-3011.

(12) Parker, D. S. N.; Zhang, F.; Kaiser, R. I., *J. Phys. Chem. A,*, **2011**, *115*, 11515-11518

(13) Albert, D. R.; Davis, H. F., *J. Phys. Chem. Lett.* , **2010**, *1*, 1107-1111.

(14) Gu, X.; Zhang, F.; Kaiser, R. I., *Chem. Phys. Lett.*, **2007**, *448*, 7-10.

(15) Fadden, M. J.; Hadad, C. M., *J Phys. Chem. A*, **2000**, *104*, 8121-8130.

(16) Merle, J. K.; Hadad, C. M., *J. Phys. Chem. A*, **2004**, *108*, 8419-8433.

(17) Frank, P.; Herzler, J.; Just, T.; Wahl, C., *Symp. Int. Combust. Proc.*, **1994**, *25*, 833 - 840.

(18) Herzler, J.; Frank, P. In *Third International Conference on Chemical Kinetics* Gaithersburg, MD, 1993; Vol. 3rd.

(19) Carpenter, B. K., *J. Am. Chem. Soc.*, **1993**, *115*, 9806-9807.

(20) Venkat, C.; Brezinsky, K.; Glassman, I., *Symp. (Int.) Combust., [Proc.]*, **1982**, *19*, 143-152.

(21) Belmekki, N.; Glaude, P. A.; Da Costa, I.; Fournet, R.; Battin-Leclerc, F., *Int J. Chem. Kinet.*, **2002**, *34*, 172 - 183.

(22) Kislov, V. V.; Singh, R. I.; Edwards, D. E.; Mebel, A. M.; Frenklach, M., *Proc. Int. Combust. Inst.*, **2014**, *Ahead of Print, DOI: 10.1016/j.proci.2014.06.135*.

(23) Kohn, D. W.; Clauberg, H.; Chen, P., *Review of Scientific Instruments*, **1992**, *63*, 4003-4005.

(24) Nicolas, C.; Shu, J.; Peterka, D. S.; Hochlaf, M.; Poisson, L.; Leone, S. R.; Ahmed, M., *J. Am. Chem. Soc.* , **2006**, *128*, 220-226.

(25) Golan, A.; Ahmed, M.; Mebel, A. M.; Kaiser, R. I., *Phys. Chem. Chem. Phys.*, **2013**, *15*, 341-347.

(26) Zhang, F.; Kaiser, R. I.; Golan, A.; Ahmed, M.; Hansen, H., *J. Phys. Chem. A*, **2012**, *116*, 3541-3546.

(27) Zhang, F.; Kaiser, R. I.; Kislov, V. V.; Mebel, A. M.; Golan, A.; Ahmed, M., *J. Phys. Chem. Lett.*, **2011**, *2*, 1731-1735

(28) Yang, J., *Photonionization Cross Section Database* *http://flame.nsrl.ustc.edu.cn/en/database.htm*, **2011**, *Version 1.0*.
(29) Li, Y., *Photonionization Cross Section Database (Version 1.0).* *http://flame.nsrl.ustc.edu.cn/en/database.htm*. , **2011**.
(30) Sander, W.; Roy, S.; Polyak, I.; Ramirez-Anguita, J. M.; Sanchez-Garcia, E., *J. Am. Chem. Soc.* , **2013**, *134*, 8222-8230.
(31) Yang, B.; Wang, J.; Cool, T. A.; Hansen, N.; Skeen, S.; Osborn, D. L., *Int. J. Mass Spectrom.*, **2012**, *309*, 118-128.
(32) Hansen, N.; Klippenstein, S. J.; Miller, J. A.; Wang, J.; Cool, T. A.; Law, M. E.; Westmoreland, P. R.; Kasper, T.; Kohse-Hoeinghaus, K., *J Phys. Chem. A*, **2006**, *110*, 4376-4388.
(33) Xu, H.; Pratt, S. T., *J. Phys. Chem. A*, **2013**, *117*, 12075-12081.
(34) Cool, T. A.; Wang, J.; Nakajiama, K.; Taatjes, C. A.; Mclllroy, A., *Int. J. Mass Spectrom.*, **2005**, *247*, 18–27.
(35) Goulay, F.; Trevitt, A. J.; Savee, J. D.; Bouwman, J.; Osborn, D. L.; Taatjes, C.; Wilson, K. R.; Leone, S. R., *J. Phys. Chem. A* **2012**, *116*, 6091−6106.
(36) Colussi, A. J.; Zabel, F.; Benson, S. W., *Int. J. Chem. Kinet.*, **1977**, *9*, 161-178.
(37) Lin, C.-Y.; Lin, M. C., *J. Phys. Chem.*, **1986**, *90*, 425-431.
(38) Buth, R.; Hoyermann, K.; Seeba, J., *Symp. (Int.) Combust., [Proc.]*, **1994**, *25*, 841-849.
(39) Liu, R. F.; Morokuma, L.; Mebel, A. M.; Liu, M. C., *J. Phys. Chem. A*, **1996**, *100*, 9314−9322.
(40) Taatjes, C. A.; Osborn, D. L.; Selby, T. M.; Meloni, G.; Trevitt, A. J.; Epifanovsky, E.; Krylov, A. I.; Sirjean, B.; Dames, E.; Wang, H., *J. Phys. Chem. A*, **2010**, *114*, 3355-3370.